Difference Spatial Distribution Function Analysis of Aqueous Solutions. IV.[1] Hydration Structure Changes of Ethylene Glycol Solutions throughout Conformational Change Process from gGg′ to tGg′ Conformers

Toshiyuki HATA and Yukio ONO*

Faculty of Pharmacy and Pharmaceutical Sciences, Fukuyama University, Sanzo, Gakuen-cho, Fukuyama, Hiroshima 729–0292, Japan. Received May 1, 2000; accepted August 11, 2000

Monte Carlo (MC) simulations were carried out for an infinitely dilute aqueous solution of two stable conformers (gGg′ and tGg′) and of three conformations between gGg′ and tGg′ conformers of ethylene glycol (EG) at 298 K. Based on the spatial distribution function (SDF) $g_{OO}(x,y,z)$, obtained from the MC simulation in the above conformations in liquid water, the high distribution of hydration water molecules could be divided into hydrogen acceptor (HA), hydrogen donor (HD), MIX (overlapped distribution of HA and HD), and hydrophobic hydration (HH) regions. The spatial orientations of hydrogen-bonded water molecules were found to be of a linear type with a triple-layer structure in the HA region and HA part (in the MIX region), and double-layer structures in the HD region and HD part (in the MIX region). In addition, it was apparent that the spatial orientations of these water molecules were of the linear type throughout the conformational change process from gGg′ to tGg′ conformers in liquid water. From the difference SDF (DSDF), $\Delta g_{OO}(x,y,z)$, between the SDFs of two conformations, we concluded that the distribution of hydration water molecules in the HA and HD parts of the MIX region are governed by the competition of internal hydrogen bonds between the hydrogen atom and two lone-pair electrons on the oxygen atom of an EG molecule.

Key words aqueous ethylene glycol solution; spatial distribution function; difference spatial distribution function; hydration structural change; conformational change

Theoretical investigations of the solvent effects on the physico-chemical properties of chemical substances and drugs are of growing importance in the study of chemical and biological reactions in solution. In order to clarify the structural geometries and physico-chemical properties of these molecules in aqueous solution, numerous researchers have carried out investigations by various molecular orbital (MO) methods and molecular mechanics.[2—4] The main approach of the MO method is reaction field theory,[5] in which solute molecules interact with a dielectric continuous medium of solvent in aqueous solution. In contrast, radial distribution function (RDF) results obtained from X-ray diffraction[6] and neutron scattering[7] methods have not suggested a homogeneous continuum structure of solvent and have shown that solvent effects cannot be reliably evaluated by the dielectric continuum model for solvent effects. Of course, molecular simulations[8] such as Monte Carlo (MC) and molecular dynamics (MD) simulations are entirely free from such approximations. However, these methods are too time-consuming to elucidate the hydration structure and solvent effect for a large solute molecule in aqueous solution.

Our studies in this series have therefore been carried out to address these problems regarding solvent effects and the calculation times required for MC simulations. First, our major goal was to develop a new method for the evaluation of solvent effects by considering the local structure of solvent water on the basis of the spatial distribution function[9] (SDF), $g_{OO}(x,y,z)$, as obtained from a MC simulation. Second, our approach was to establish the optimal construction method for SDF when applied to the hydration structure of a large molecular system by employing the SDFs of fundamental small molecular systems obtained from an MC simulation.

In general, it is considered that many chemical and biological molecules exist in a state formed by internal and/or external hydrogen bonds in aqueous solution. In addition, based on the results of NMR measurements, it has been reported that the molecular conformations that make possible the formation of internal and/or external hydrogen bonds in apolar solvent differ significantly from the conformations in polar solvent, and that it is the polar solvent water that is primarily responsible for the induction of this change in molecular structure.[10] Therefore, we consider that it is very important to clarify the anisotropic hydration structures and solvent effects of such a molecule.

To succeed in our above approach, we adopted ethylene glycol (EG) as the simplest compound having two kinds of hydrogen bonds. The EG molecule is particularly hydrophilic due to its two hydroxyl groups, which are used as both hydrogen acceptor (HA) and hydrogen donor (HD) in hydrogen bonds with solvent water molecules. An interesting question arises regarding the hydration structure of various stable conformers based on the internal hydrogen bond between two adjacent hydroxyl groups and the external hydrogen bond with solvent water molecules. The EG molecule builds up a three-dimensional network of external hydrogen bonds with solvent water in aqueous EG solution, which suggests the existence of a variety of stable conformers based on the dihedral angle changes of the EG molecule. These conformers of EG are identified by the three O1–C1–C2–O2, H1–O1–C1–C2, and H2–O2–C2–C1 dihedral angles, and the central O1–C1–C2–O2 dihedral angle is denoted by a capital letter (*e.g.*, gGg′ and tGg′ in Chart 1). The capital letter G indicates a conformation with a *gauche* position in the central dihedral angle. The symbols g, t, and g′ represent *gauche* (+synclinal), *trans* (antiperiplanar), and *gauche′* (−synclinal), as defined by Radom *et al.*, respectively.[11]

* To whom correspondence should be addressed. e-mail: ono@fupharm.fukuyama-u.ac.jp

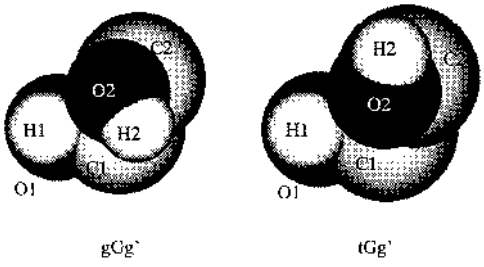

Chart 1. Two Conformers of Ethylene Glycol

Experimental studies on the conformational equilibrium of the EG molecule have been reported, *e.g.*, results measured by electron diffraction,[12] infrared (IR),[13] and microwave (MW)[14] spectroscopic methods. On the other hand, several researchers have theoretically investigated the conformational equilibrium of the EG molecule using various calculation methods.[15—17] Cramer and co-workers[16] have reported that the results at various levels of *ab initio* MO and semi-empirical MO calculations are consistent with experimental results. They have therefore concluded that populations (over roughly 95%) of *gauche* conformers (capital letter G) in the central dihedral angle for the equilibrium gas phase and aqueous solution at 298 K are much larger than those (within roughly 5%) of *trans* conformers. In addition, they have found that two *gauche* conformers (gGg′ and tGg′) with internal hydrogen bonds make up approximately 70—84% of the overall conformers in the gas phase and in aqueous solution. On the other hand, Nagy *et al*.[17] have investigated the hydration structures of gGg′, tGg′, g′Gg′, and tTt conformers in aqueous solutions by means of the radial distribution function (RDF) obtained from a Monte Carlo (MC) simulation. However, the three-dimensional hydration structure and its change throughout the conformational change process in aqueous EG solution have not yet been characterized using an MC simulation.

In this investigation, we adopted the gGg′ and tGg′ conformers shown in Chart 1, and three conformations between gGg′ and tGg′ conformers. The respective five conformations in infinitely dilute aqueous solution are hereafter referred to as their respective conformations in liquid water.

This paper describes the following results for the SDF $g_{OO}(x,y,z)$, difference SDF (DSDF), $\Delta g_{OO}(x,y,z)$, proposed in our previous paper, and the binding energy (BE) of the five conformations in liquid water. First, the anisotropic hydration structures around an EG molecule were analyzed using the SDF $g_{OO}(x,y,z)$ obtained from an MC simulation for two conformers (gGg′ and tGg′) of EG in liquid water. Second, the difference in solvation energy between gGg′ and tGg′ was evaluated from the BE. Third, it was shown that the hydration structure changes of EG molecules throughout the conformational change process can be characterized by the DSDF $\Delta g_{OO}(x,y,z)$ between the SDFs for two conformations in liquid water.

Computational Procedure

Monte Carlo Simulation MC simulations[8] were carried out for all systems with one EG molecule and 215 water molecules in a cube with a cell length of 18.63 Å within the Metropolis scheme[18] in the NVT ensemble at 298 K. The molar volume obtained under the liquid water density of 1.0 g cm^{-3} was 18.015 cm^3 mol^{-1}.

As described in our previous papers,[1] SPC potential[19] and TIPS potential[20] functions were employed to represent the intermolecular interactions for water, and for alcohol and ether, respectively. These potential functions were obtained from the sum of the Coulomb and Lennard–Jones terms as:

$$\Delta E = \sum_{i}^{\text{in } A} \sum_{j}^{\text{in } B} (q_i q_j e^2 / r_{ij} + A_{ij} / r_{ij}^{12} - C_{ij} / r_{ij}^{6})$$

The coefficients, A_{ij} and C_{ij}, were obtained from $\sqrt{A_{ii} \times A_{jj}}$ and $\sqrt{C_{ii} \times C_{jj}}$, respectively. The interatomic distance and bond angle values for water were r(OH)=1.0 Å and ∠HOH=109.47°. These values for the EG molecule were r(OH)=0.945 Å, r(CO)=1.430 Å, r(CC$_O$)=1.512 Å, ∠COH=108.5°, and ∠CCO=107.8°. The dihedral angles optimized by *ab initio* MO methods using MP2/6-31G** were ∠H2–O2–C2–C1=72.86°, ∠O1–C1–C2–O2=55.43°, and ∠H1–O1–C1–C2=−42.19° for the gGg′ conformer and ∠H2–O2–C2–C1=−165.79°, ∠O1–C1–C2–O2=60.04°, and ∠H1–O1–C1–C2=−50.79° for the tGg′ conformer.[15e] The dihedral angles adopted in the MC simulation were ∠H2–O2–C2–C1=70°, ∠O1–C1–C2–O2=60°, and ∠H1–O1–C1–C2=−50° for the gGg′ conformer and ∠H2–O2–C2–C1=−170°, ∠O1–C1–C2–O2=60°, and ∠H1–O1–C1–C2=−50° for the tGg′ conformer (Chart 1). The conformational change process from gGg′ to tGg′ conformers could easily be examined by this model. Further, in order to visualize the hydration structure changes throughout the conformational change process from the gGg′ to tGg′ conformers, three conformations for the dihedral angle, ∠H2–O2–C2–C1=100, 130, and 160°, were calculated by the MC simulation. These geometries were fixed in the MC simulation. In the SDF calculation, the O1 atom, O1–C1 bond, and H1 atom lie on the origin of the coordinate, the x-axis, and the direction of y-axis, respectively. Therefore, three atoms, H1–O1–C1, lie on the x–y plane. After excluding the first 2500000 configurations, the subsequent 5000000 configurations were employed to obtain the statistical average in the MC simulations.

Difference Spatial Distribution Function Bosio *et al*.[21] have reported the temperature dependence of hydration structures using the difference radial distribution function (DRDF) for heavy water obtained from X-ray diffraction. They have described that the network structure of the hydration water decreases with rising temperature. In a previous paper,[1] we proposed a new DSDF method for examining the effects of hydrophobic groups. This DSDF is obtained as the difference between the SDFs for two states calculated by the MC simulation. For example, the DSDF, $\Delta g_{OO}(x,y,z)$, for two conformations of EG molecules with the dihedral angle ∠H2–O2–C2–C1=130° and 160° is determined as:

$$\Delta g_{OO}(x,y,z) = g_{OO}(x,y,z)_{160^\circ \text{ EG}} - g_{OO}(x,y,z)_{130^\circ \text{ EG}}.$$

Binding Energy Decomposition The binding energy (BE)[22] is obtained as the sum of all spatial cells of the coefficient products calculated from the volume and coordination number (CN), the SDF $g_{OO}(x,y,z)$, and the averaged potential energies $\langle E(x,y,z)\rangle$ between the solute and solvent molecules at a certain point in a cubic cell. Applying the linked-list clustering technique, the high-density distributions of the SDF $g_{OO}(x,y,z)$ for oxygen (solute)–oxygen (solvent) pairs appeared to fall in one of three different regions, that of a hydrogen acceptor (HA), a hydrogen donor (HD), or a hydrophobic hydration (HH). The BE are calculated for each region using the next equation. For example, the value of the BE for the HA region in alcohol solution is determined by:

$$\langle BE \rangle_{\text{HA}} = \sum_{x,y,z \in \text{HA}} \frac{N}{V} \times \Delta V \times \langle E(x,y,z) \rangle \times g_{OO}(x,y,z)$$

where N is the number of water molecules in the cube with a cell length of 18.63 Å, V is the volume of a cube, and ΔV is an infinitesimal volume. In addition, $\langle BE \rangle_{\text{Sum}}$ can be obtained as the sum of $\langle BE \rangle_{\text{x}}$ for the above three regions, HA, HD, and HH.

Results and Discussion

Hydration Structure The anisotropic hydration structures of water molecules around EG molecule could be visualized by SDF $g_{OO}(x,y,z)$ using the graphic display technique. With regard to the gGg′ and tGg′ conformers in liquid water, Fig. 1 shows the distributions of SDF $g_{OO}(x,y,z)$=2.1 between solute and water molecules as obtained from the MC simulation at 298 K. As shown in Fig. 1, the high distrib-

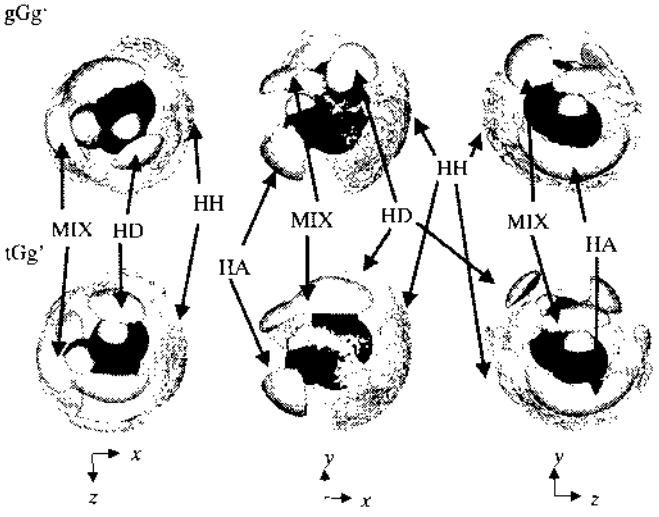

Fig. 1. Isosurfaces of Oxygen (Solute)–Oxygen (Water) SDF $g_{OO}(x,y,z)=2.1$

Isosurfaces for top and bottom lines of the figure are shown for gGg′ and tGg′ conformers, respectively. Left, middle, and right columns are isosurfaces viewed down the *y*-axis, *z*-axis and *x*-axis, respectively.

Table 1. Results of Volume, CN, and Binding Energy Decomposition for gGg′ and tGg′ Conformers of Ethylene Glycol in Liquid Water in $g_{OO}(x,y,z)\geqq 2.1$ Region at 298 K

	gGg′			tGg′		
	Volume	CN	$\langle BE\rangle_x$	Volume	CN	$\langle BE\rangle_x$
HA	7.2	0.92	−16.77	7.1	0.93	−17.81
HD	3.2	0.69	−12.85	3.4	0.62	−9.88
MIX +HH	23.1	2.25	−18.24	21.8	2.11	−14.91
Sum	33.5	3.86	−47.86	32.3	3.66	−42.60
Total			−113.59			−102.68

Units for volumes and $\langle BE\rangle_x$ are Å^3 and kJ mol^{-1}, respectively. Subscript x on $\langle BE\rangle_x$ indicates HA, HD, MIX, Sum, and Total. $\langle BE\rangle_{Total}$ means the BE obtained from the overall cubic cell.

utions of SDF $g_{OO}(x,y,z)$ for the hydration water molecules around the EG molecule could be classified into the HA, HD, and HH regions; as the results for our previously reported alcohol solutions are also shown. A new overlapped distribution also appears in the area of the internal hydrogen bond of EG. This overlapped distribution composed of HA and HD regions is hereafter referred to as the MIX region. The distributions of the HA and HD regions for the two stable conformers, gGg′ and tGg′, are very similar to the SDF in all alcohol solutions reported previously. On the other hand, the ethylene portion of the molecule is surrounded by a distribution of hydration water molecules in the HH region, and the distribution area of this HH region is spread out in the vicinity of the distribution of the MIX region.

Applying the linked list clustering technique,[23] the high distributions of SDF $g_{OO}(x,y,z)\geqq 2.1$ for oxygen (solute)–oxygen (water) pairs fall into three different regions: HA, HD, and (MIX+HH) regions. Table 1 shows the volume, CN, and BE ($\langle BE\rangle_x$) for each region of SDF $g_{OO}(x,y,z)\geqq 2.1$, and BE ($\langle BE\rangle_{Total}$) for all spatial regions in a cubic cell in aqueous EG solution at 298 K. It is considered that the results of this clustering technique characterize the hydration structures of the first hydration shell, because this SDF $g_{OO}(x,y,z)\geqq 2.1$ is more than twice that for the bulk state ($g_{OO}(x,y,z)=1.0$).

As shown in Table 1, in the HA region, the volume and CN values in the gGg′ conformer in liquid water were 7.2 Å^3 and 0.92, and these values in the tGg′ conformer in liquid water were 7.1 Å^3 and 0.93. The $\langle BE\rangle_{HA}$ (−17.81 kJ mol^{-1}) in the latter was more stable than that (−16.77 kJ mol^{-1}) in the former. In the HD region, the volume and CN values in gGg′ conformer were 3.2 Å^3 and 0.69, and those values in the tGg′ conformer water were 3.4 Å^3 and 0.62. The $\langle BE\rangle_{HD}$ (−12.85 kJ mol^{-1}) in the former was considerably smaller than that (−9.88 kJ mol^{-1}) in the latter. In the (MIX+HH) region, the volume and CN values in the gGg′ conformer were 23.1 Å^3 and 2.25, and those values in the tGg′ conformer were 21.8 Å^3 and 2.11. The $\langle BE\rangle_{(MIX+HH)}$ (−18.24 kJ mol^{-1}) in the former was appreciably smaller than that (−14.91 kJ mol^{-1}) in the latter. These results indicate that the solvation energy increases with increasing CN values of hydration water molecules for each region.

From the $\langle BE\rangle_{Sum}$ and $\langle BE\rangle_{Total}$ values in Table 1, the energy differences in these values for two conformers, gGg′ and tGg′, in liquid water appear to have been 5.26 and 10.91 kJ mol^{-1}, respectively. These results indicate that solvation effect for gGg′ conformer is greater than that for tGg′. In addition, our results support the results reported by Nagy *et al.*,[17] Hooft *et al.*[24] and Cramer and co-workers.[16] It is apparent from these results that $\langle BE\rangle_{HD}$ and $\langle BE\rangle_{(MIX+HH)}$ are the primary contributors to the solvation energy for gGg′ conformer in liquid water.

Figure 2 shows contour maps of the BE on the *x*–*y* plane $z=0.075$ Å in gGg′ and tGg′ conformers in liquid water. As can be clearly seen, the maps of the BE for the HA and HH regions in gGg′ conformer are very similar to those for the same regions in tGg′ conformer. In the HA region, the distributions of stable BE in gGg′ and tGg′ conformers are spread out in the vicinity centered at $x=-1.4$ Å and $y=-2.3$ Å, and the negative value (−2.0 kJ mol^{-1}) in this field indicates the existence of a stable area. The distributions of stable BE (−2.0 kJ mol^{-1}) in the HH region are also spread out in the vicinity centered at $x=5.0$ Å and $y=-1.0$ Å, although the distributions of unstable BE in two conformers are spread out on the side of the solute molecule. These contour maps for the HA and HH regions in two conformers are in agreement with those of alcohol solutions. In the other two distributions of stable BE in gGg′ conformer, the distribution of stable BE is spread out in the vicinity centered at $x=-1.1$ Å and $y=2.8$ Å, corresponding to the MIX region based on the distribution of HA and HD regions, because the distribution of stable BE in the vicinity centered at $x=3.2$ Å and $y=4.1$ Å is assigned to the HD region formed by hydrogen bonds between solvent water and the H2 atom of EG. In contrast, the widespread distribution in the tGg′ conformer corresponds to the MIX region formed by the overlap of the HA and HD regions. Taken together, these contour maps also suggest that the MIX region is formed by the overlap of HA and HD regions relating to the O2 and H1 atoms of EG, respectively.

Figure 3 shows a superposition of oxygen–oxygen and oxygen–hydrogen SDFs, $g_{OO}(x,y,z)$ and $g_{OH}(x,y,z)$, in gGg′ and tGg′ conformers in liquid water. This figure shows that the hydration structures of the hydrogen-bonded water form a triple-layer structure in the HA region and HA part (in MIX), and a double-layer structure in the HD region and the HD

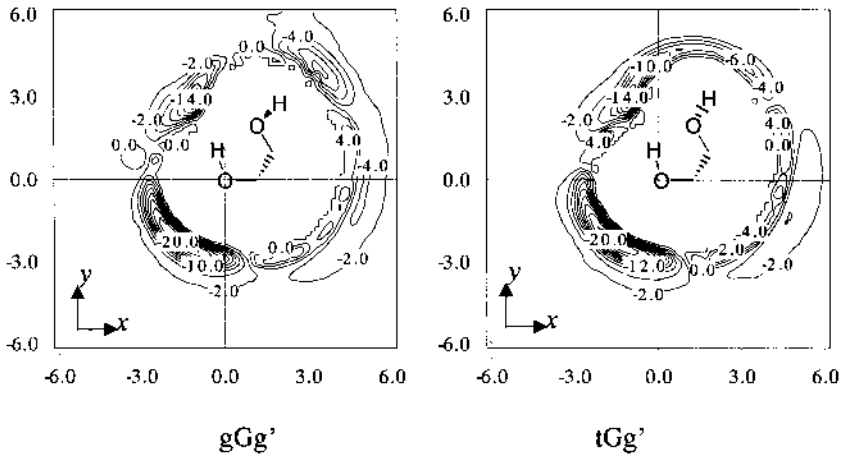

Fig. 2. Contour Maps of Binding Energies for gGg′ and tGg′ Conformers on the x–y Plane of $z=0.075$ Å at 298 K

Energy increment between two neighboring contour lines is 2 kJ mol^{-1}.

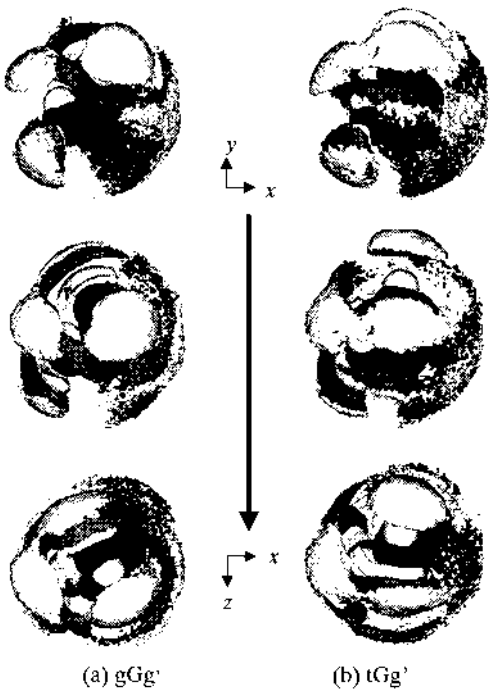

Fig. 3. Superposition Representations of Oxygen (Solute)–Oxygen (Water) and Oxygen (Solute)–Hydrogen (Water) SDF for (a) gGg′ and (b) tGg′ Conformers in Liquid Water at 298 K

The dark area shows the oxygen–oxygen distribution at $g_{OO}(x,y,z)=2.1$, and the bright area shows the oxygen–hydrogen distribution at $g_{OH}(x,y,z)=1.6$. The top and bottom lines of the figure are superposition representations viewed down the z-axis and y-axis, respectively.

part (in MIX). Distribution peak distances between the H (or O) atom of solvent water molecules and the O (or H) atom of EG in five conformations are shown in Table 2. From Fig. 3 and Table 2, in the HA region, the maximum distributions of hydrogen, oxygen, and hydrogen atoms in hydration water molecules occur at distances of approximately 1.7, 2.8, and 3.3 Å from the O1 atom of gGg′ and tGg′ conformers, respectively. In the HD region, the maximum distributions of oxygen and hydrogen atoms in water molecules occur at distances of approximately 1.9 and 2.3—2.4 Å from the H2 atom of gGg′ and tGg′, respectively. Therefore, it is evident that the triple-layer and double-layer structures are composed of each maximum distribution in the HA and HD regions, respectively.[1)] On the other hand, in the MIX region, the maximum distributions in the vicinity of the O2 atom of EG occur at distances of approximately 1.8 (hydrogen), 2.8 (oxygen), and 3.2—3.3 (hydrogen) Å from the O2 atom of gGg′ and tGg′. Moreover, the maximum distributions in the vicinity of the H1 atom of EG also occur at distances of approximately 1.9—2.0 (oxygen) and 2.4 (hydrogen) Å from the H1 atom of gGg′ and tGg′. From these distribution distances, the hydration structures in the MIX region also appear to have formed triple-layer and double-layer structures. From the water dimer structures optimized by our *ab initio* MO calculation,[1a)] these spatial orientations of triple-layer and double-layer structures appear to be of all the linear type. Taken together, these findings clearly indicate that triple-layer and double-layer structures are composed of each maximum distribution in the HA region and HA part (in MIX) regions in the vicinity of the O2 atom, and the HD region and HD part (in MIX) regions in the vicinity of the H1 atom, respectively. Then, except in the case of the HH region, we can conclude that the spatial orientations of the hydration water molecules for all regions in the first hydration shell are of the linear type. Moreover, the isosurface of SDF and the superposition representation of the SDFs shown in Figs. 1 and 3 indicate that the distribution in the MIX region is in agreement with the overlapped distribution composed of the HA part relating to the O2 atom and the HD part relating to the H1 atom of the EG molecule.

Hydration Structure Changes throughout the Conformational Change Process from gGg′ to tGg′ Conformers As mentioned above, the equilibrium populations of both gGg′ and tGg′ in all conformers are approximately 70—84% in aqueous solution.[16)] Therefore, from the SDF and DSDF, we analyzed an anisotropic hydration structure change throughout the conformational change process from gGg′ to tGg′ conformers.

First, we determined the transition state and the conformational change pathway between gGg′ to tGg′ conformers of the EG molecule using the MNDO-AM1 method[25)] with eigenvector following[26)] and an intrinsic reaction coordinate,[27)] respectively. Table 3 shows three dihedral angles of the EG molecule at the pathway of the conformational

Table 2. Distribution Peak Distances between Tow Atoms of Solvent Water Molecules and Five Conformations of Ethylene Glycol (EG) in Liquid Water

EG Water	O1			O2			H1		H2	
	H	O	H	H	O	H	O	H	O	H
gGg′	1.7	2.8	3.3	1.8	2.8	3.2	1.9	2.4	1.9	2.4
100°	1.7	2.8	3.3	1.8	2.9	3.3	2.0	2.4	1.9	2.3
130°	1.7	2.8	3.3	1.8	2.8	3.2	2.0	2.4	1.8	2.4
160°	1.7	2.8	3.3	1.9	2.8	3.3	2.0	2.2	1.9	2.2
tGg′	1.7	2.8	3.3	1.8	2.8	3.3	2.0	2.4	1.9	2.3

Units for all values are Å.

Table 3. Dihedral Angle Changes Accompanying Conformational Change from gGg′ to tGg′ Conformers of Ethylene Glycol

Reaction Coordinate	gGg′	−2	−1	TS	1	2	tGg′
H2–O2–C2–C1	73.2	81.7	108.9	133.0	143.4	166.4	175.4
O1–C1–C2–O2	62.6	62.6	62.4	62.7	63.0	63.8	64.2
H1–O1–C1–C2	−47.5	−48.9	−51.6	−53.5	−53.9	−55.2	−55.8

Transition state, TS, are found by MNDO-AM1 method with eigenvector following, and conformational change path are obtained from MNDO-AM1 method with intrinsic reaction coordinate. Units for all values are degree.

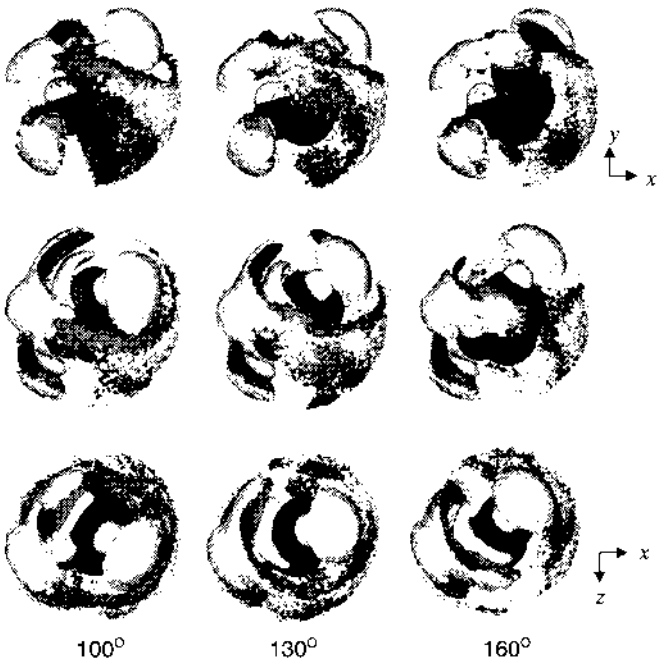

Fig. 4. Superposition Representations of Oxygen (Solute)–Oxygen (Water) and Oxygen (Solute)–Hydrogen (Water) SDF for 100°, 130°, and 160° Conformations in Liquid Water at 298 K

The dark area shows the oxygen–oxygen distribution at $g_{OO}(x,y,z)=2.1$, and the bright area shows the oxygen–hydrogen distribution at $g_{OH}(x,y,z)=1.6$. The top and bottom lines of the figure are superposition representations viewed down the z-axis and y-axis, respectively.

change. As shown in Table 3, it is apparent that the dihedral angle for each conformational change significantly with only ∠H2–O2–C2–C1, and ∠O1–C1–C2–O2 and ∠H1–O1–C1–C2 remaining unaltered. This result indicates that the conformational change from gGg′ to tGg′ can be expressed as the variation of the rotation angle around the H2 atom of EG.

Then, we proposed five conformations at 70 (gGg′), 100, 130, 160, and 190° (tGg′) for the dihedral angles ∠H2–O2–C2–C1, and the hydration structure in each conformation in liquid water was analyzed by SDFs obtained from the MC simulation at 298 K. Figure 4 shows a superposition of SDFs, $g_{OO}(x,y,z)$ and $g_{OH}(x,y,z)$, for each conformations. Moreover, the distances between the high distributions of oxygen (or hydrogen) atoms of solvent water and hydrogen (or oxygen) atoms of solute EG are shown in Table 2. As clearly seen in Fig. 4 and Table 2, the maximum distributions of hydrogen, oxygen, and hydrogen atoms in the hydration water molecules in the HA region occur at distances of approximately 1.7, 2.8, and 3.3 Å from the O1 atom of the EG molecule, respectively. In the HA part (in MIX) based on the O2 atom of EG, these distributions occur at distances of approximately 1.8—1.9, 2.8—2.9, and 3.2—3.3 Å, respectively. Therefore, it is evident that the triple-layer structure is composed of each maximum distribution in the HA region and HA part (in MIX region), and that their spatial orientations are of a linear type.

On the other hand, the maximum distributions of oxygen and hydrogen atoms in the hydration water molecules in the HD region occur at distances of approximately 1.8—1.9 and 2.2—2.4 Å from the H2 atom of EG, respectively. In the HD part (in MIX) based on the H1 atom of EG, these occur at distances of approximately 1.9—2.0 and 2.2—2.4 Å, respectively. Therefore, it is evident that the double-layer structure is composed of each maximum distribution in the HD region and HD part (in MIX), and that their spatial orientations are also of a linear type. Taken together, we can conclude that the hydration structure around EG continually holds both the triple-layer structure in the HA region and the double-layer structure in the HD region throughout the conformational change process from gGg′ to tGg′ conformers.

Except in the case of the HH region, Table 4 shows the volume, CN, and BE ($\langle BE\rangle_x$) in the HA, HD, and MIX regions for SDF $g_{OO}(x,y,z)\geqq 2.5$ in EG in liquid water at 298 K. Compared with the SDF $g_{OO}(x,y,z)\geqq 2.1$ in the (MIX+HH) region in Table 1 and SDF $g_{OO}(x,y,z)\geqq 2.5$ in the MIX region in Table 4, the difference BE (-4.77 kJ mol^{-1}) between the BEs of the former and the latter for the gGg′ conformer was approximately 30% that of the BE of the former, with 10, 5, and 15% contributions from the

Table 4. Results of Volume, CN, and Binding Energy Decomposition for Five Conformations of Ethylene Glycol in Liquid Water in $g_{OO}(x,y,z)\geqq 2.5$ Region at 298 K

		gGg′				tGg′
		70°	100°	130°	160°	190°
HA	Volume	5.6	6.1	6.0	5.8	5.6
	CN	0.81	0.89	0.87	0.83	0.82
	$\langle BE\rangle_x$	−15.06	−17.06	−16.94	−16.47	−16.04
HD	Volume	2.6	2.8	2.7	2.8	2.8
	CN	0.65	0.59	0.58	0.57	0.58
	$\langle BE\rangle_x$	−12.29	−10.46	−9.76	−9.43	−9.35
MIX	Volume	7.1	6.0	5.8	4.9	6.0
	CN	1.06	0.89	0.77	0.70	0.93
	$\langle BE\rangle_x$	−13.47	−11.54	−8.98	−8.43	−10.92

Units for volumes and $\langle BE\rangle_x$ are Å^3 and kJ mol^{-1}, respectively. Subscript x on $\langle BE\rangle_x$ indicates HA, HD, and MIX.

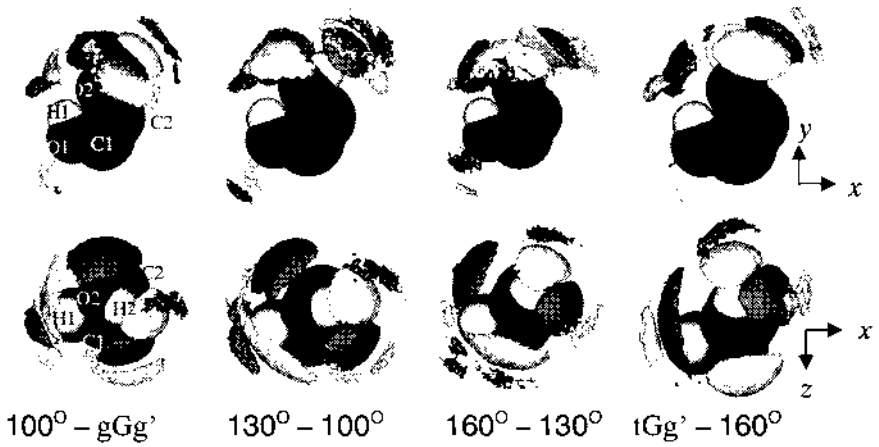

Fig. 5. Isosurfaces of Difference Oxygen (Solute)–Oxygen (Water) SDF between Two Conformations in Liquid Water

The top and bottom lines of the figure are isosurfaces viewed down the *z*-axis and *y*-axis, respectively. The bright area shows the increase of oxygen–oxygen distribution at $\Delta g_{OO}(x,y,z)=+1.0$, and the dark area shows the decrease of oxygen–oxygen distribution at $\Delta g_{OO}(x,y,z)=-1.0$.

HA, HD, and HH regions, respectively, contributions that remained constant throughout the conformational change process from gGg′ to tGg′. Based on the above, it appears that the influence of the HH region connected with that of the MIX for the hydration structure may be less than that of the HA, HD, and MIX regions.

As seen clearly in Table 4, the volume and CN in the HA and HD regions didn't change as significantly as expected, but the BE in these regions varies appreciably with the conformational change. On the other hand, all of these values in the MIX region vary significantly with the conformational change. These results indicate that the hydration structure change is most strongly dependent on the MIX region relative to the HA and HH regions.

The origin of these effects can easily be determined using our novel DSDF method. Figure 5 shows an isosurface of DSDF $\Delta g_{OO}(x,y,z)=\pm 1.0$ obtained from SDFs of two conformations. As can clearly be seen, however, the high distribution area based on the H2 atom is appreciably shifted with the rotational transfer of the H2 atom. In addition, the high distribution areas of the hydration water molecules in the HD region relative to the H2 atom and in the HA region based on the O1 atom are practically unaltered.

If the conformational change pathway proceeds from gGg′ to tGg′, the high distribution of hydration water molecules in the HA part (in MIX region) can be classified into two high distributions of solvent water with lone-pair electrons on the O2 atom with and without internal hydrogen bonds formed by the H1 atom. The former distribution increased as the conformational change proceeded from gGg′ to tGg′, while the latter decreased. These distribution changes could have been due to the internal hydrogen bond of the lone-pair electrons on the oxygen atom with the H1 atom, *i.e.*, a disappearance in the former process and an appearance in the latter one. This result indicates that the distribution for the HA part (in MIX) decreases as the internal hydrogen bond formed by the H1 atom is enhanced and increases as this bond is weakened. To the contrary, however, it is apparent that the distribution for the HD part (in MIX), based on the behavior of the H1 atom, increase as the internal hydrogen bond formed by the H1 atom is enhanced. Considering the above, we have concluded that the hydration structure change is primarily governed by the contribution of the MIX region relative to that of the HA and HD regions

Conclusion

In the present paper, we have analyzed hydration structures and their changes throughout the conformational change process in aqueous EG solution using the SDF $g_{OO}(x,y,z)$ and our novel DSDF $\Delta g_{OO}(x,y,z)$ methods, respectively.

From the results of the SDF $g_{OO}(x,y,z)$ for five conformations of EG in liquid water at 298 K, it became apparent that the hydration water molecules for the first hydration shell are primarily distributed in the HA, HD, and MIX (an overlapped distribution of the HA and HD parts connected by an internal hydrogen bond) regions. These distributions show a triple-layer structure in the HA region and the HA part (in the MIX region), and a double-layer structure in the HD region and the HD part (in MIX region), and the spatial orientations of the hydration water molecules in these regions are obviously of a linear type. In addition, it became apparent that the spatial orientation of the hydration water molecules remains of a linear type throughout the conformational change process from gGg′ to tGg′ conformers.

In terms of the results of the DSDF $\Delta g_{OO}(x,y,z)$ obtained from the SDFs $g_{OO}(x,y,z)$ for the two conformations in liquid water, it was noted that the distribution of hydration water molecules in the HA and HD parts (in MIX region) are governed by the competition of internal hydrogen bonds between the H1 atom and the two lone-pair electrons on the O2 atom. More specifically, in the MIX region, the high distribution of hydration water molecules for the HA part related to the O2 atom decreases as the internal hydrogen bond formed by the H1 atom is enhanced, while that for the HD part increases as the hydrogen bond is enhanced.

In order to investigate in more detail the hydration structure around amino and carboxyl groups containing biologically important amino acid, we are presently examining MC simulations of amine and carboxylic acid solutions.

References

1) *a*) Hata T., Ono Y., *Chem. Pharm. Bull*., **47**, 615—620 (1999); *b*) *Idem*, *ibid*., **48**, 16—20 (2000); *c*) *Idem*, *ibid*., **48**, 957—963 (2000).
2) Miertuš S., Scrocco E., Tomasi J., *Chem. Phys*., **55**, 117—129 (1981).
3) Hoshi H., Sakurai M., Inoue Y., Chûjô R., *J. Chem. Phys*., **87**, 1107—1115 (1987).
4) Klanmt A., Schüürmann G., *J. Chem. Soc*., *Perkin Trans. 2*, **1993**, 799—805.
5) Still W. C., Tempczyk A., Hawley R. C., Hendrickson T., *J. Am. Chem. Soc*., **112**, 6127—6129 (1990).
6) Narten A. H., Danford M. D., Levy H. A., *Discuss. Faraday Soc*., **43**, 97—107 (1967).
7) Soper A. K., Phillips M. G., *Chem. Phys*., **107**, 47—60 (1986).
8) Allen M. P., Tildesley D. J., "Computer Simulation of Liquids," Oxford University Press, New York, 1987.
9) *a*) Svishchev I. M., Kusalik P. G., *J. Chem. Phys*., **99**, 3049—3058 (1993); *b*) Kusalik P. G., Svishchev I. M., *Science*, **265**, 1219—1221 (1994); *c*) Svishchev I. M., Kusalik P. G., *J. Chem. Phys*., **100**, 5165—5171 (1994); *d*) Liu Q., Brady J. W., *J. Am. Chem. Soc*., **118**, 12276—12286 (1996); *e*) Laaksonen A., Kusalik P. G., Svishchev I. M., *J. Phys. Chem. A*, **101**, 5910—5918 (1997); *f*) Bergman D. L., Laaksonen L., Laaksonen A., *J. Mol. Graphics*., **15**, 301—306 (1997); *g*) Pitera J., Kollman P., *J. Mol. Graphics.*, **15**, 355—358 (1997).
10) *a*) Lossli H.-R., Kessler H., Oschkinat H., Weber H.-P., Petcher T. J., Widmer A., *Helv. Chimi. Acta*, **68**, 692—704 (1985); *b*) Wegner R. M., France J., Bovermann G., Walliser L., Widmer A., Widmer H., *FEBS Lett*., **340**, 255—259 (1994).
11) Radom L., Lathan W. A., Hehre W. J., Pople J. A., *J. Am. Chem. Soc*., **95**, 693—698 (1973).
12) Bastiansen O., *Acta Chem. Scand*., **3**, 415—421 (1949).
13) *a*) Frei H., Ha T.-K., Meyer R., Günthard H. H., *Chem. Phys*., **25**, 271—298 (1977); *b*) Takeuchi H., Tasumi M., *ibid*., **77**, 21—34 (1983).
14) *a*) Caminati W., *J. Mol. Spectrosc*., **86**, 193—201 (1981); *b*) Caminati W., Corbelli G., *ibid.*, **90**, 572—578 (1981).
15) *a*) Ikuta S., Nomura O., *Chem. Phys. Lett*., **154**, 71—76 (1989); *b*) Costa Cabral B. J., Albuquerque L. M. P. C., Silva Fernandes F. M. S., *Theor. Chim. Acta*, **78**, 271—280 (1991); *c*) Murcho M. A., DiPaola R. A., *J. Am. Chem. Soc*., **114**, 10010—10018 (1992); *d*) Teppen B. J., Cao M., Frey R. F., van Alsenoy C., Miller D. M., Schafer L., *J. Mol. Struct*. (*Theochem*.), **314**, 169—190 (1994); *e*) Reiling S., Brichkmann J., Schlenkrich M. Bopp P. A., *J. Comput. Chem*., **17**, 133—147 (1996); *f*) Costa Cabral B. J., *Int. J. Quantum Chem*., 1651—1660 (1996).
16) Cramer C. J., Truhlar D. G., *J. Am. Chem. Soc*., **116**, 3892—3900 (1994).
17) Nagy P. I., Dunn W. J., III, Alagona G., Ghio C., *J. Am. Chem. Soc.*, **113**, 6719—6729 (1991).
18) Metropolis N., Rosenbluth A. W., Rosenbluth M. N., Teller A. H., Teller E., *J. Chem. Phys*., **21**, 1087—1092 (1953).
19) Berendsen H. J. C., Grigera J. R., Straatsma T. P., *J. Phys. Chem*., **91**, 6269—6271 (1987).
20) Jorgensen W. L., *J. Am. Chem. Soc*., **103**, 335—340 (1981).
21) Bosio L., Chen S.-H., Teixeira J., *Phys. Rev. A*, **27**, 1468—1475 (1983).
22) Ben-Naim, "Water and Aqueous Solutions, Introduction to a Molecular Theory," Chapter 5, Plenum Press, 1974.
23) Ōsawa E., Gotō H., Hata T., Deretey E., *J. Mol. Struct*. (*Theochem*.), **398**—**399**, 229—236 (1987).
24) Hooft R. W. W., van Eijck B. P., Kroon J., *J. Chem. Phys*., **97**, 3639—3646 (1992).
25) Dewar M. J. S., Zoebisch E. G., Healy E. F., Stewart J. J. P., *J. Am. Chem. Soc.*, **107**, 3902—3909 (1985).
26) Baker J., *J. Comp. Chem*., **7**, 385—395 (1986).
27) Dieter K. M., Stewart J. J. P., *J. Mol. Struct*. (*Theochem*), **163**, 143—149 (1988).